Increasing the radar ATR system performances by using a modified version of fuzzy integral applied on HRR and video imaginary

Iulian-Constantin VIZITIU, Petrică CIOTÎRNAIE

***Abstract*—** One of the most often used tools to increase the performances of automatic target recognition system is the fusion technique (data or decision fusion). In the current study we investigated the possibility of improving the version of the standard Sugeno's fuzzy integral. Moreover, in order to constantly increase the performances of radar ATR system, we have applied the above mentioned decision fusion method on datasets designed by using high-resolution radar and video imaginary. For the finality of this study, in order to confirm the theoretical aspects, a real input database was used.

***Keywords*—**radar ATR system, standard fuzzy integral, fuzzy-evolutive integral, HRR and video imaginary

I. INTRODUCTION

FOR the purpose of practical radar target classification, only three promising techniques proper to be implemented into operational radar systems are mentioned in the specialized literature. According to [1] and [2], these techniques are: *inverse synthetic aperture radar* (ISAR), *jet engine modulation* (JEM) and respectively, *high-resolution radar range profiles* (HRRP). Recently, a lot of scientific research works has been focussed on the use of HRRP, since this method allows the possibility of increasing the performances of radar target classification.

The *high resolution radar* (HRR) is able to relieve the reflectivity characteristic of a target, i.e. the positioning of its scattering points [3]. On the other hands, the radar bandwidth required for these waveforms is in the range of GHz.

The HRRP techniques are often used in the radar ATR system. According to [4], HRRP offers the possibility of target classification from all points of view. The collection of HRRPs implies only a short radar dwell *time on target* (TOT), since no coherent integration is required. A HRRP can always be collected, whereas ISAR and JEM require special condition for data acquisition. HRRPs are not compulsory recommended for radar system operator interpretation, therefore automated classification procedures (ATR) are also required. Generally, HRRPs may provide an excellent radar signature for target classification, and their guaranteed availability makes them very useful when other techniques such as ISAR or JEM are not available. A very useful and comprehensive comparison between the radar ATR techniques can be found in [4].

Generally speaking, a range profile of a target can be considered as its radar 1D signature, generated by the reflection of a high-frequency broadband electromagnetic signal. This is obtained by the projection of the target scattering points, defining the *high-resolution chart of target* on the *radar line of sight* (RLOS) [5]. Fig.1 depicts an example of a radar target profile (ideal and real HRRP).

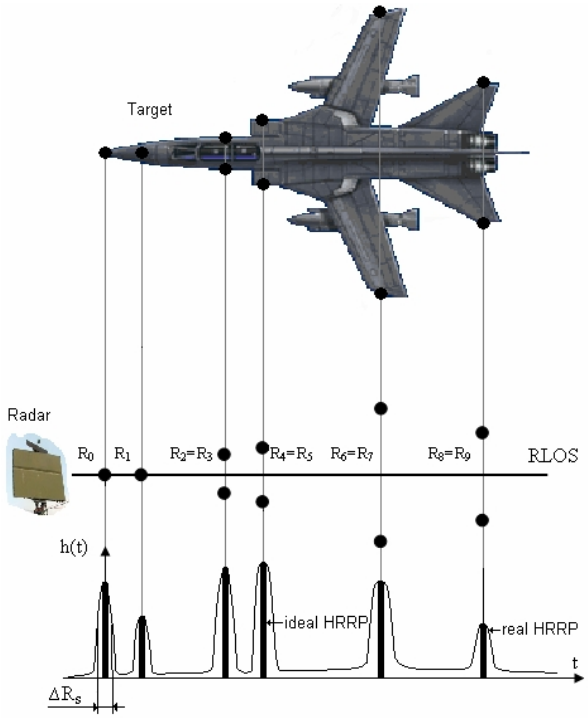

Fig.1 Example of a radar target range profile (HRRP)

In the specialized literature assigned to radar ATR system theory based on HRRP use, a lot of methods for radar pattern recognition are mentioned. The most part of these approaches starts from the basic target 1D HRRP processing [6], [7], [8] but the usage of target HRR *imaginary* from the perspective of

Manuscript received May 29, 2007. This work was supported by CNCSIS (Romania) under Grant AT 115/88GR (2006-2007) 'Design of smart multisensor system for automatic air target tracking and recognition'. Revised received November 15, 2007.

I.C.Vizitiu is with the Communications and Electronic System Department, Military Technical Academy, Bucharest, CO 040531 Romania (corresponding author to provide phone: +4021-335-4660; fax: +4021-335-5763; e-mail: vic@ mta.ro).

P.Ciotîrnaie is with the Communications and Electronic System Department, Military Technical Academy, Bucharest, CO 040531 Romania (corresponding author to provide phone: +4021-335-4660; fax: +4021-335-5763; e-mail: ciotirnaie@ mta.ro).

recognition level can be more effective [9], [10], [11]. However, the classification results offered by all these methods depend on the specific procedure used for target HRRP reconstruction, on the radar information accuracy and perturbation factor influence [2], [6].

According to [12], the more information is available, the more effective the ATR process is. Consequently, a very good option would be the use of information gathered from several (spectral independent) sensors for *high level fusion* (or *decision fusion*). Starting from the actual quality of the provided information and classification process, that is specific to video imaginary, a *fusion set* of imaginary type {HRR, video} can be very interesting for further ATR system implementation.

Fusion makes the (radar) ATR system not only more powerful, but also more robust since different spectral sensors have specific capabilities and robustness in regard to the perturbation factors.

Several standard models are presented in the literature, in order to implement the decision fusion [9], [11]. However, the main problem of these methods is the developing of efficient algorithms to combine the answers from various classifiers in order to get the best results. According to this, other much more systematic approaches are based on the possibility theory, on the Dempster-Shafer theory, fuzzy logic or Sugeno's fuzzy integral [11], [12].

The main goal of this study is to propose a suitable design solution for a more efficient ATR system, based on improved version of Sugeno's standard fuzzy integral, and on target HRR and video imaginary decision fusion use, respectively.

Our proposed solutions in the current study will be checked by using a real database. Therefore, a theoretical approach of the standard and improved fuzzy integral algorithms is done in the first part of the paper. Then we will describe the design procedure for the real database used in unrolled applications. In the result section, are shown the experimental results that confirm the broached theoretical approaches from beginning. At the end of the paper, some conclusions and future research directions in this action field are included.

II. STANDARD FUZZY INTEGRAL

Sugeno's fuzzy integral represents a non-linear functional, similar to a Lebesgue's integral, defined with respect to a fuzzy measure [11], [12].

Let us consider a set Q, and $h: Q \to [0,1]$ representing a fuzzy subset of Q. The standard fuzzy integral of the function *h* on Q, with respect to the fuzzy measure *g*, is expressed by the equation:

$$\int_Q h(q) \circ g(\cdot) = \max_{A \subseteq Q} \left[\min \left[\min_{q \in A} \left(h(q), g(A) \right) \right] \right] = \max_{\alpha \in [0,1]} \left[\min \left(\alpha, g(h_\alpha) \right) \right], \quad (1)$$

where $h_\alpha = \{ q \,|\, h(q) > \alpha \}$.

Function $h(q)$ quantifies the decision taken by the classifier q concerning the membership of the unknown target to some class. In other words, the value of $h(q)$ function measures the degree with which the concept *h* is satisfied by *q*.

The term $\min_{q \in A} h(q)$ measures then the degree with which the concept *h* is satisfied by all the elements of the subset *A*. Function $g(A)$ represents the relevance of the classifier group constituting the set *A* for the final decision or, in an similar way, the degree with which they satisfy the concept *g*. Consequently, the value obtained by the comparison of the two quantities through the operator *min* will indicate the degree with which the classifier set *A* satisfies the two criteria.

Based on above mentioned ideas, one can then conclude that the fuzzy integral looks for the maximum degree of agreement between the real possibilities and expectations, measured by the function *h* and *g*, respectively.

In order to calculate the standard fuzzy integral, the values $h(q_i)$ are supposed to be sorted in descending order: $h(q_1) \geq h(q_2) \geq ... \geq h(q_N)$. If they are not in the intended order, one can always change the order of q_i, so that this condition is satisfied. Hence, the fuzzy integral can be calculated using the following equation:

$$\chi = \int_Q h(q) \circ g(\cdot) = \max_{i=\overline{1,N}} \left[\min \left(h(q_i), g(A_i) \right) \right], \quad (2)$$

where $A_i = \{ q_1, q_2, ..., q_i \}$.

Function $g(A_i)$ can be calculated in an iterative way using the basic property of any fuzzy measure g_l :

$$\begin{cases} g(A_i) = g(\{q_1\}) = g^1 \\ g(A_i) = g^i + g(A_{i-1}) + l \cdot g^i \cdot g(A_{i-1}), \; i = \overline{2,N} \end{cases}. \quad (3)$$

According to [13], the decision fusion of the *N* outputs of the *N* classifiers is then carried out by the standard algorithm presented in Fig.2.

A. Training stage

S1. Measure the performances of the classifiers and get their fuzzy density function for each class.

Term $g_j^i = g_j(\{q_i\})$ is considered to be the *classification rate* (CR) assigned to classifier q_i for the class C_j.

(cont.)

S2. Calculate, for each class C_j, the corresponding value λ_j by using the equation:

$$g(Q)=1\Rightarrow \lambda+1=\prod_{i=1}^{N}\left(1+\lambda g_j^i\right). \quad (4)$$

B. Classification stage

S1. Calculate the outputs $o_j^i=h_j(q_i)_{j=\overline{1,m},i=\overline{1,N}}$ of the *N* classifiers corresponding to the *m* classes.

S2. Calculate the fuzzy integral for each class considering $g_j(A_i)$ given by equation (1):

$$\chi=\max_{i=\overline{1,N}}\left[\min\left(o_j^i, g_j(A_i)\right)\right]. \quad (5)$$

S3. Decide on the membership of the target according to the rule:

$$\begin{cases}\text{if } \max\limits_{j=\overline{1,m}}\chi_j\geq\chi_0 \text{ and } k=\arg\left(\max\limits_{j=\overline{1,m}}\chi_j\right)\Rightarrow x\in C_k\\ \text{if } \max\limits_{j=\overline{1,m}}\chi_j\leq\chi_0\Rightarrow \text{unknown target}\end{cases}, \quad (6)$$

where χ_0 indicates a confidence threshold below which the target is declared unknown. It can be considered as the lowest value of the fuzzy integral χ_k obtained during the training process.

Fig.2 Working algorithm of standard fuzzy integral

The block diagram describing the fusion procedure using Sugeno's standard fuzzy integral is also presented in Fig.3.

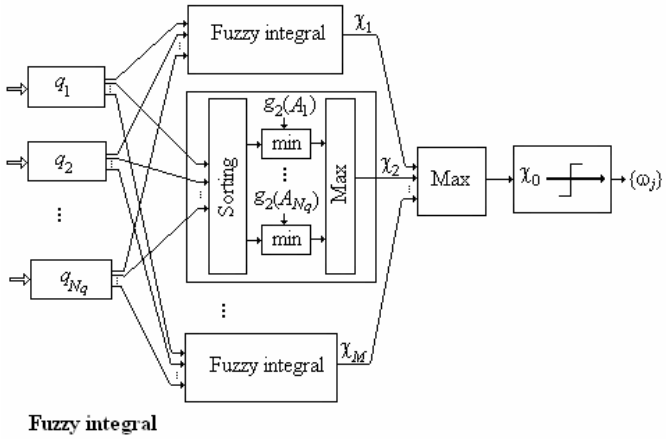

Fig.3 Decision fusion based on standard Sugeno's fuzzy integral usage

More details regarding standard fuzzy integral theory can be found in [13].

III. FUZZY-EVOLUTIVE INTEGRAL

The *fuzzy-evolutive* integral is a hybrid method used to optimize the mixing mode of the outputs assigned to more (neural) classifiers. This procedure uses the standard fuzzy integral to realise the suitable output combination of some distinctive neural networks based on importance assigned those by a proper genetic algorithm.

Consequently, the chromosomes will *real* encode the fuzzy densities g_i^j as a $C_j=\left(g_1^j, g_2^j, ...; \lambda_j\right)$ vector, and the *fitness* function for C_j is given by equation:

$$E(C_j)=\sum_{A\in B(X)}\left|g_{\lambda_e}(A)-\frac{1}{\lambda_j}\left[\prod_{x_i\in A}\left(1+\lambda_j g_i^j\right)-1\right]\right|, \quad (7)$$

where $\left\{g_{\lambda_e}(A)\right\}$ are the initial assigned values for fuzzy measures, and $\left\{g_{\lambda_e}(A)\right\}$ are the calculated values using g_i^j and λ_j.

Fig.4 depicts the basic diagram describing the proposed fusion method.

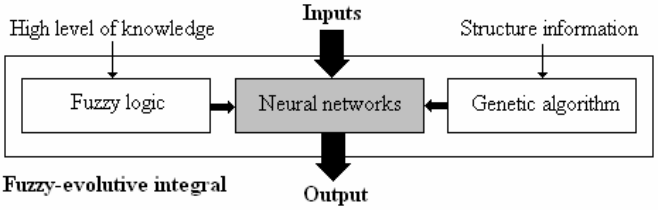

Fig.4 Decision fusion based on fuzzy-evolutive integral usage

The *stopping criterion* for the used genetic algorithm was represented by exceeding of the maxim generation number (which has a constant value), or by reaching of the goal error.

The *parents selection* for the next generation was realized using an *elitist* method. In order to eliminate untimely convergence phenomenon, the *fitness* function was scaled according to the following equation:

$$E_{\max}^{new}=k\cdot E_{\max}^{old},\ k\in[1.2,2] \quad (8)$$

The *crossover* has suppossed the use of two splitting points (randomly chosen), and each chromosome had attached a certain crossover probability with values in the range of $[0.6-0.95]$. In order to introduce new chromosomes into the current population, and to protect genetic algorithm against irreversible and accidental information failures generated by improper crossover operations, the *mutation* was used. The

probability of mutation was chosen in the range of $[0.001-0.01]$.

Generally speaking, it is well known that the solution given by genetic algorithm is coded under the form of the most performant chromosome that belongs to the last generation, but in fact nothing garantees us that a more performant chromosome has been obtained, for example, in the previous chromosomial generation.

Consequently, using the analogy with the *Gallant* algorithm from neural network theory [15], the best chromosom from this population at each chromosomial generation will be kept and indexed into *pocket*, and thus after a suitable decreasing order technique, will really result the best final solution.

More details regarding fuzzy-evolutive integral theory and assigned genetic algorithm can be found in [13] and [14].

IV. DATABASE DESIGN

In order to add more consistency to applications developed in the experimental part of this paper, the database was made by using the actual information given by *two* spectral independent sensors: one sensor in *visible* spectrum (a CCD camera), and another radar sensor (by ISAR type).

Accordingly to this, the database used will contain the following *two* target image datasets:

A. Video dataset

As one can see on Fig.5, the video dataset was obtained by using a (digital) photographical survey of *five* military aircraft models (F 117, Mirage 2000, Mig 29, F16 and Tornado) scaled at 1:48 (see Fig.5a).

The survey was taken by using a 5^0 increment in the azimuthal plane, into the angular range of $\left[0^0-180^0\right]$, justified by the geometric aircraft shape symmetry.

F 117 Mirage 2000

(a) Examples of aircraft models used in video database design

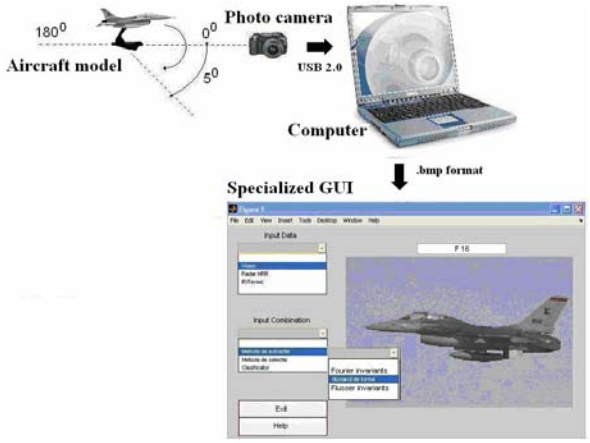

(b) Acquisition and pre-processing stage

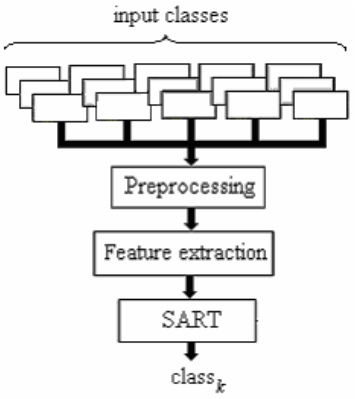

(c) Classification stage

Fig.5 Basic diagram used in case of video dataset design

Each image from the input video database has a resolution of 520×160 pixels in an uncompressed BMP format.

After the acquisition and pre-processing step (see Fig.5b), a number of 37 video images per class is obtained. The modified Flusser invariants [16], [17] were used as feature extraction method. The feature vector matrix has the dimension of (11×37) for each involved target.

B. HRR (HH and VV) datasets

The HRR image reconstruction algorithm (for the same military aircrafts) contains the following basic *steps*:

1) *Primary radar data acquisition and HRRP generation*

The real data were obtained in an anechoic chamber using the experimental setup shown in Fig.6.

Each target was illuminated in the acquisition phase with a stepped frequency signal. The data snapshot contains 128 frequency steps, uniformly distributed over the band $[11-65,8]$ GHz, which results in a frequency increment of $\Delta f = 50$ MHz. Accordingly, the slant range resolution and ambiguity window are given by the equation bellow:

$$\Delta R_S = \frac{c}{2B} \cong 3\,\text{m},\ W_S = \frac{c}{2\Delta f} \cong 2.35\,\text{cm}. \qquad (9)$$

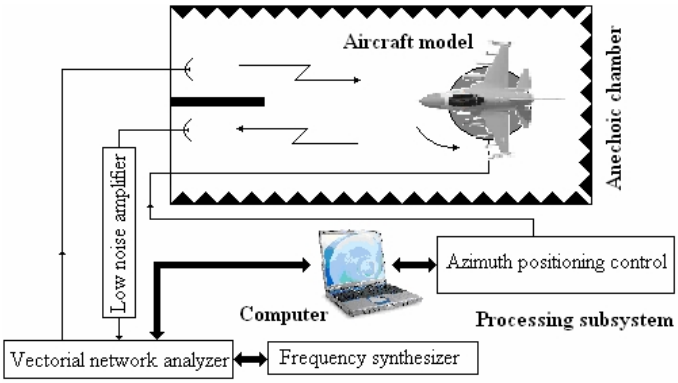

Fig.6 Experimental setup

The *frequency* (*complex*) *signature* obtained from a backscattered snapshot is coherently integrated by using IFFT transformation in order to obtain the slant HRRP (HH and VV) corresponding to a given aspect of an involved target. For each out of the 5 targets, 201 range profiles for 201 angular

positions are thus generated, between -5^0 and 95^0, with an angular increment of 0.5^0. Therefore, for each involved target, the HRRP matrix has the dimension of (128×201).

2) *Target HRR image reconstruction*

Using spectral analysis in polar coordinates for measured complex samples, the reflection point projection on a plane perpendicular on the target rotation axis, i.e. target radar image (or HRR image) can be obtained.

If the argument sampling is uniform, we can apply Fourier-2D transformation to the measured dataset. As one can see on Fig.7a, this is valid in Cartesian coordinates but it is not in polar coordinates (b,f). Therefore, the primary input data interpolation in Cartesian system (k_x, k_y) is necessary. Thus, the target HRR image can be obtained applying e.g., Fourier-2D transformation on interpolated data set (see Fig.7b).

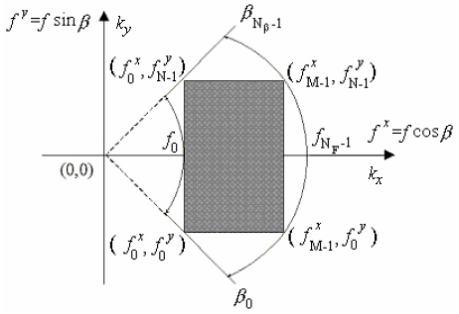

(a) Resampling technique for reformatting radar data from polar to Cartesian coordinates

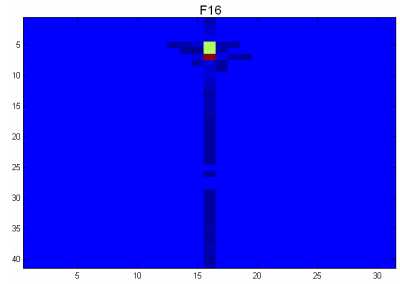

F16 military aircraft

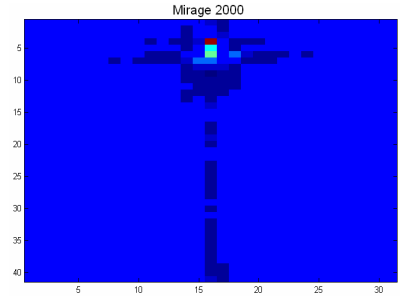

Mirage 2000 military aircraft

(b) Examples of target HRR images obtained by applying the Fourier-2D

Fig.7 Target HRR image reconstruction using Fourier-2D

3) *Final form of HRR image dataset*

According to [9], applying Fourier-2D transformation on the HRRP set is not a very good solution to generate target HRR image. It has no good influence on ATR system performance level, as well. However, a more efficient solution, and in the same time as well as more robust concerning the action of noise for classification step, is represented by super resolution algorithms, e.g. 2D-MUSIC, 2D-ESPRIT etc. when applying them on the interpolated dataset.

In order to generate a single target HRR image (see Fig.8), the HRRP from a 10^0 angular sector was used. After using ESPRIT-2D algorithm, we obtained the 19 HRR images/class. The *polygonal contour* that results using a suitable reunion of the target detected reflection points is interesting enough for the classification step.

Finally, using a feature extraction algorithm similar with the one from video image case, it clearly results that, for each involved target, the feature vector matrix has the dimension of (11×19).

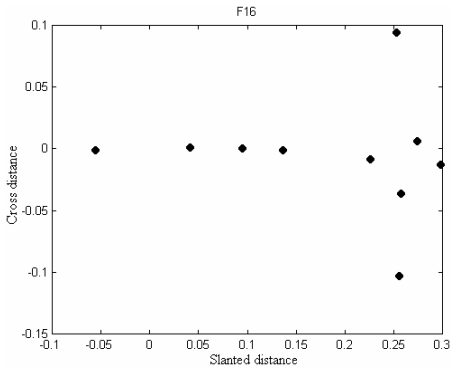

F16 military aircraft

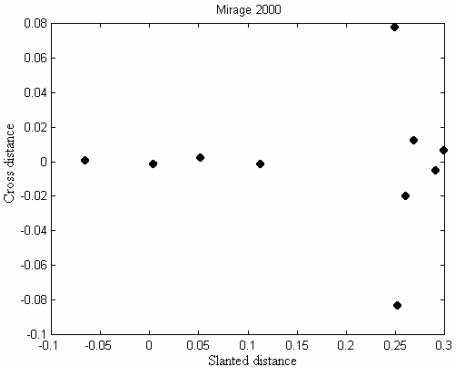

Mirage 2000 military aircraft

Fig.8 Example of target HRR images obtained by ESPRIT-2D applying

More details regarding HRR and video database design can be found in [13].

V.EXPERIMENTAL RESULTS

The main *objectives* of these experiments are:

1) to demonstrate that the usage of the modified version of the standard Sugeno's fuzzy integral leads to improved classification results for radar ATR system;

2) to demonstrate that the usage of the decision fusion between video image dataset and HRR image datasets results in more increased classification rates than in the case of 1D HRRP or HRR imaginary singular use.

In order to finalize the recognition system form, after feature extraction step and for each input class, an interlacing splitting algorithm was applied on resulted matrix. Accordingly, in case

of feature matrix with the dimension of (11×37), a number of 19 vectors were used for classifier training while for testing 18 vectors were used. Finally, a *supervised ART artificial neural network* (SART) was used for classification purposes (see Fig.5b).

According to [10] and [15], SART classifier is developed using q* standard algorithm. A set of prototypes, which approximates the probability density modes of the vectors of each input class, was used. The *nearest neighbour* (NN) classification rule is then used to classify the new vectors as compared to these prototypes. Generally speaking, this classifier generates in a *supervised* manner a new prototype if the distance between the new vector and the existing prototype exceeds a certain threshold (according to *Follow the leader* principle from ART artificial neural network theory).

Each class $C_j = \left\{ x_k^{(j)} \right\}_{k=\overline{1,N_j}}$ is represented by one or several prototypes $\left\{ p_k^{(j)} \right\}_{k=\overline{1,P_j}}$, which approximate the modes of the underlying *probability density function* (PDF), where N_j and P_j represent the number of vectors and of the prototypes corresponding to the class j. The prototypes are equivalent to the codebook vectors used by the VQ techniques, or to the centers used by the RBF training algorithms.

According to [13], the SART training algorithm starts by randomly setting of one prototype for each class. The basic idea is to create a new prototype for a class whenever the actual set of prototypes is not able to satisfactorily classify the input training data set using the NN rule:

$$\left\| x - p_l^{(i)} \right\| = \min_{j=\overline{1,M},k=\overline{1,N_j}} \left\| x - p_k^{(j)} \right\| \Rightarrow x \in C_i. \quad (9)$$

If, for example, the vector x previously classified do not actually belongs to the class C_i, but to another class, say C_r, then a new prototype $p_{N_r+1}^{(r)} = x$ will be added to the list of prototypes already assigned to class C_r. The prototypes are updated during each epoch by using the mean of the samples, which are correctly classified by the corresponding prototypes:

$$p_l^{(i)} = \frac{1}{\operatorname{card}\left\{ A_l^{(i)} \right\}} \sum_{x_m \in A_l^{(i)}} x_m, \quad (10)$$

where $A_l^{(i)} = \left\{ x_m^{(i)} \middle| \left\| x_m^{(i)} - p_l^{(i)} \right\| = \min_{j,k} \left\| x_m^{(i)} - p_k^{(j)} \right\| \right\}$.

A prototype does not account for a minimum number of training vectors (typically 1) is canceled because it is supposed to represent outliers:

$$\operatorname{card}\left\{ A_l^{(i)} \right\} \le N_l \Rightarrow p_l^{(i)} \text{ is canceled.} \quad (11)$$

The updating process is repeated as long as the classification errors on the training samples still exist, and as long as dynamically changes the location of the prototypes. Also, the SART classifier can be easily fitted with a neural network structure in a very similar manner to the LVQ or RBF neural networks (see Fig.10) [13], [15].

Consequently, Fig.9 exibits the standard algorithm of SART neural classifier.

A. Initialization stage

S1. Select randomly as prototype a vector for each class from input space.

S2. Initialize the vector list associated to each class prototype.

B. Learning stage

S1. As long as the prototypes change and the error rate is higher than a preset value, and for each vector belonging to an input class, compare and classify this vector with the actual prototype list.

If the input vector is correct classified, add the vector to the list assigned to the winner prototype.

If the vector is not correct classified, declare the vector as new prototype and update the initial vector list.

Update the prototypes assigned to each class. Recalculate the prototypes as an average between the vectors that are associated with its own list.

Check whether or not some current prototypes have changed.

Eliminate the prototypes for which the associated vector list contains only a vector.

Exit when the number of maxim iterations or prototypes is reached.

S2. Calculate the neuronal weights of the output layer using the *pseudo-inverse* method, or *Widrow-Hoff* algorithm [15].

Fig.9 Working algorithm of SART classifier

Finally, the block diagram describing the internal working algorithm of SART classifier is also presented in Fig.10.

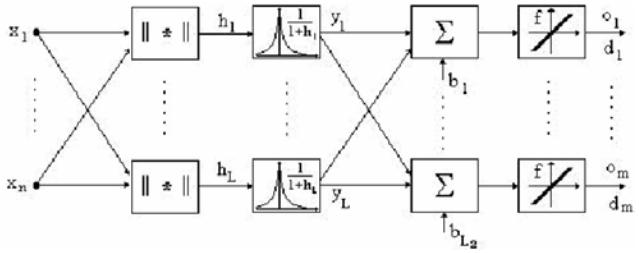

Fig.10 SART classifier internal structure

In the case of using a HRR dataset, the classification stage is quite similar with the one described above, and the resulted matrix has the dimension of (11×19). Also, a number of 10

feature vectors were used for SART classifier training while for testing 9 feature vectors were used.

In order to quantify and compare the classification results, the CR (*classification rate*) has been computed (it represents the most important performance indicator). The significance of CR (in %) is the ratio between the number of correct classified input patterns and the total number of the patterns used.

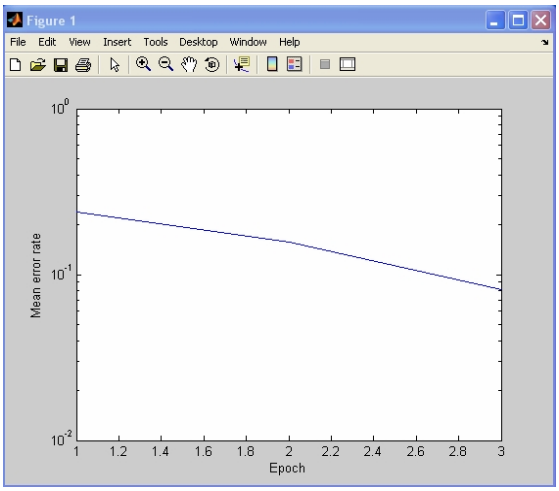

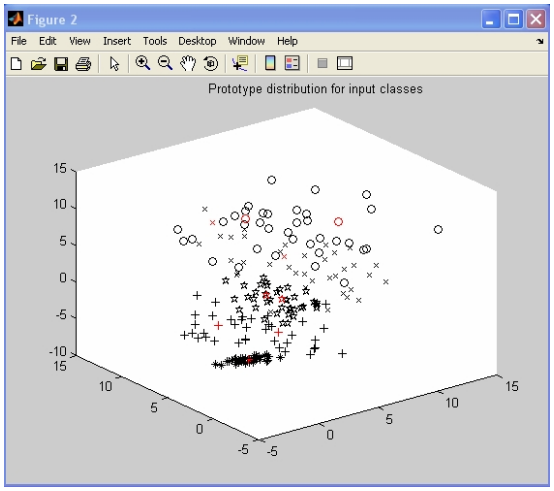

(a) Specific diagrams assigned to SART classifier training stage

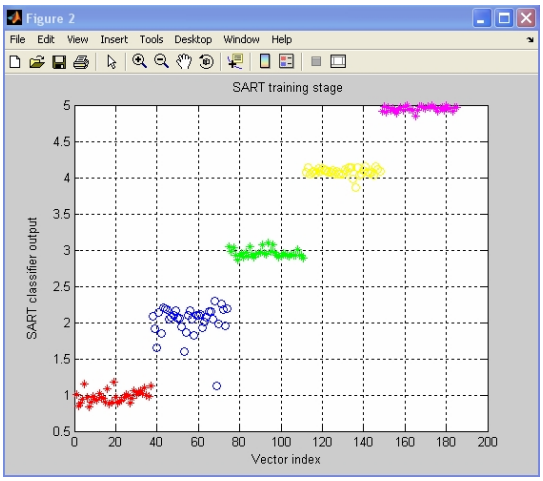

(b) Classification result presentation (used for CR calculus)

Fig.11 Classification results in case of video database usage

Using HH and VV HRR datasets, and after a comparative study between two types of decision fusion models, the classification results are synthetically presented in Table I.

TABLE I
CLASSIFICATION RESULTS AFTER COMPARATIVE STUDY

Dataset	Classification rate, CR (%)					
	F117	Mirage	Mig 29	F16	Tornado	$\overline{M}$
HRR/HH input dataset	92	85	87	94	92	**90**
HRR/VV input dataset	91	92	86	92	93	**91**
Standard fuzzy integral	94	93	92	97	95	**94**
Fuzzy-evolutive integral	97	97	94	100	96	**97**

Also, after applying standard Sugeno's fuzzy integral, its output value variation is indicated in Fig.12.

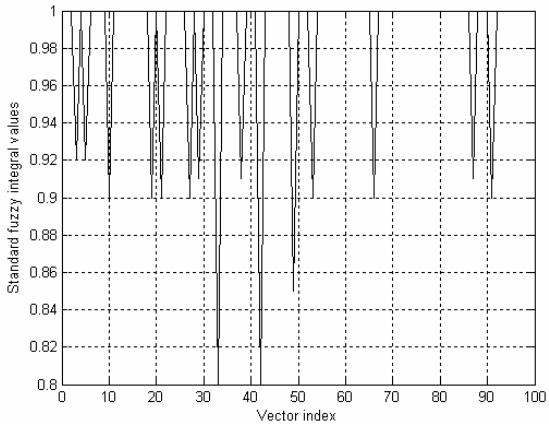

Fig.12 Standard fuzzy integral values during decision fusion

As one can see in Table I, the proposed modified version of the fuzzy integral has higher values of CR than the standard fuzzy integral.

Adding the video dataset to the HRR datasets, and by using the improved version of Sugeno's fuzzy integral, we obtained the experimental results shown in Table II.

TABLE II
CLASSIFICATION RESULTS AFTER VIDEO DATASET ADDITION

Dataset	Classification rate, CR (%)					
	F117	Mirage	Mig 29	F16	Tornado	$\overline{M}$
HRR/HH input dataset	92	85	87	94	92	**90**
HRR/VV input dataset	91	92	86	92	93	**91**
Video input dataset	95	92	94	95	95	**94**
Fuzzy-evolutive integral	100	98	96	100	99	**99**

As one can see from Table II, usage of the new input dataset and applying fuzzy-evolutive integral lead to higher values of CR than the dataset based only on HRR imaginary use.

All applications presented in this section were developed using MATLAB™ toolboxes *Nnet* and *Image processing*.

Also, in order to implement the proposed genetic algorithm for Sugeno's fuzzy integral optimization, *GAOT* toolbox was used on a Pentium ™ processor at 2.4 GHz.

More details regarding experimental aspects treated in this section can be found in [12] and [13].

VI. CONCLUSION AND FUTURE WORK

The theoretical and experimental results in this paper lead to the following *remarks* concerning the method proposed in order to increase the efficiency of radar ATR systems:

1) using the proposed decision fusion method, as well as HRR imaginary, the CR is improved, generally by 3%, as compared to the standard fuzzy integral;

2) adding video imaginary to the HRR imaginary, as well as applying the evolutive version of standard fuzzy integral, the CR is also improved, generally by 2%, as compared to the singular usage of target HRR image;

3) as a result of applying the last decision fusion model, the resulting classification rates are similar with the ones indicated in the literature [7], [8], [11], [12], i.e. more than 95%;

4) the computing resources required for fuzzy-evolutive integral calculus are similar with those from the case of standard fuzzy integral use because the genetic optimization of fuzzy densities is not a very expensive time process.

Summarizing, an ATR system that will use the proposed algorithm will be more *effective*, and will have an improved spectral *robustness* at perturbation action.

The comparative study between presented fusion decision models is intended to be will extended for the case of noisy HRRPs used in the reconstruction of target HRR image. It is very important also to analyze and quantify the influence on ATR system classification performances of SNR or relative error of reflection point positioning.

Another interesting point for a further development refers to the design of entirely new neural classification algorithms, which means more robust neural networks for feature extraction and selection, and for 2D or 3D target classification using different types of imaginary, particularly HRR imaginary.

Finally, in the same scientific research direction it will be interesting to make a thoroughly experimental analysis concerning the design and use of more performing imaginary sensor combinations (e.g. IR, thermal or video L^3).

REFERENCES

[1] Nebabin V.G., *Methods and Techniques of Radar Recognition*, Artech House, London, 1994

[2] P. Tait, *Introduction to Radar Target Recognition*, UK: IEE Radar, Sonar and Navigation series, no. 18, 2005

[3] Wehner R., *High Resolution Radar*, Artech House, Boston, 1987

[4] A. Zyweck, "Preprocessing Issues in High Resolution Radar Target Classification", Ph. D. thesis, The University of Adelaide, Mar. 1995

[5] E.Radoi, "3D object recognition using electromagnetic signature", Ph.D. thesis, ENSIETA, Brest, France, Jun. 1999

[6] I.C. Vizitiu and L. Anton, "Radar target recognition using range profile", in *Proc. of Int. Conf. on Military Informational Systems. EW and Data Security*, 2005, pp. 263-266

[7] B. Chen, H. Liu, and Z. Bao, "An Efficient Kernel Optimization for Radar High-Resolution Range Profile Recognition", *EURASIP Journal on Advances in Signal Processing*, vol. 2007, article ID 49597, 2007

[8] A.P. Szabo, and P.E. Lawrence, "Target classification using high-resolution range profile", in *Defence Application of Signal Processing*, DSTO Publications, 2005

[9] I.C. Vizitiu, I.Nicolaescu and P.Ciotirnaie, "Target Recognition Improvement Using the Decision Fusion between HRR and Video Imaginary", in *Proc. of Int. Conf. NAUN Communications and Information Technology*, 2008, Marathon, Greece, pp. 241-246

[10] A. Quinquis, E. Radoi, and F.Totir, "Some radar imagery results using supperresolution techniques", *IEEE Transactions on Antennas and Propagation*, vol. 52, no. 5, pp. 1230-1244, 2004

[11] A. Martin and E. Radoi, "Effective ATR Algorithms Using Information Fusion Models", in *Proc. of the 7th Int. Conf. on Information Fusion*, 2004, pp. 161-166

[12] I.C. Vizitiu, "An Application of Fuzzy Integral concerning the Recognition Performance Increase of Neural Missile Homing System", in *Proc. of 4th Int. Conf. on Radar and ELINT/ESM Systems*, 2007

[13] I.C. Vizitiu, "Video Pattern Recognition using Neural Networks", Ph.D. thesis, MTA, Bucharest, Romania, Nov. 2003

[14] I.C. Vizitiu, *Genetic algorithms for neural network optimization*, MTA Publishing House, Bucharest, 2005

[15] R.O. Duda, P.O. Hart, and D.G. Stork, *Pattern Classification*, New York, USA: John Wiley&Sons, 2001

[16] I.C.Vizitiu, D.Munteanu, "A new version of Flusser moment set for pattern feature extraction ", in *Proc. of 6th Int. Conf. WSEAS CIMMACS*, 2007, Tenerife, Spain, pp.456-461

[17] J. Adams, E. Curtis, "Feature Extraction Methods for Form Recognition Applications", in *WSEAS Transactions on Information Science and Applications*, vol.3, issue 3, pp.666-671, 2006